Thermal neutron detection by entrapping ^{6}LiF nanocrystals in siloxane scintillators

2015 J. Phys.: Conf. Ser. 620 012010

(http://iopscience.iop.org/1742-6596/620/1/012010)

Thermal neutron detection by entrapping ^{6}LiF nanocrystals in siloxane scintillators

SM Carturan[1,2], T Marchi[2], G Maggioni[1,2], F Gramegna[2], M Degerlier[1,3], M Cinausero[2], M Dalla Palma[2,4], A Quaranta[2,4]

[1]University of Padova, Department of Physics and Astronomy, Padova, Italy.
[2]INFN - Laboratori Nazionali di Legnaro, Italy.
[3]Nevsehir Hacı Bektas Veli University, Science and Art Faculty Physics Department, Nevsehir Turkey.
[4]University of Trento, Department of Industrial Engineering, Trento Italy.

E-mail: carturan@lnl.infn.it, saramaria.carturan@unipd.it

Abstract. Exploiting the long experience in design and production of scintillating mixtures based on siloxane matrices with combinations of primary dye and waveshifter, a first set of ^{6}LiF loaded scintillator disks has been produced. The synthesis is herein described and reported, as well as preliminary results on their light response towards thermal neutrons. The preservation of transparency and mechanical integrity of the scintillator material is challenging when introducing the inorganic salt LiF which is a "foreign body" to the organic polysiloxane host matrix. Different strategies such as synthesis of nanoparticles and surface functionalization have been pursued to succeed in the entrapment of the neutron converter whilst maintaining moderate light output, optical transparency and flexibility of the base scintillator.

1. Introduction

The importance of revealing nuclear weapons concealed in trucks or boats at the borders, using Radiation Portal Monitors (RPM) has grown up, unfortunately, in the last years. Furthermore, there is a renewed interest in neutron detection both in nuclear physics, mainly related to the development of Radioactive Ion Beam facilities, and in applied physics related fields, such as materials analysis by neutron imaging and diffraction spectroscopy.

The use of ^{3}He for the detection of moderated neutrons with almost full rejection of γ-rays generated events has become prohibitive, due to the exceedingly high price/liter of this rare isotope, though the reliability of ^{3}He-based systems is still unrivalled. This has triggered a widespread and intensive research work aimed at ^{3}He replacement. Systems based on scintillators, both inorganic [1] and organic [2-5] have been recently proposed as neutron detectors, while compact and robust silicon based detectors where neutron converter thin films are used for signal generation have been recently ideated and proved their excellent performances [6]. Siloxane-based scintillators are, in principle, very simple and economic tools for particle detection. Their capability to detect thermal neutrons by loading with ortho-carborane has been demonstrated, but the limited solubility of the organoboron compound hampered their further development [7].

Other neutron converters have been tried as dopants for siloxane, such as Gd and Cd, but the toxicity of Cd itself and the intrinsic emission of γ-rays following neutron capture on Gd or Cd make those systems less attractive than ^{6}Li doped scintillators. In this case, the triton and alpha particles from the ^{6}Li reaction, as detailed by Knoll [8], can differently excite the material with respect to γ-rays, thereby enabling n-γ discrimination by pulse shape analysis (PSA).
In this preliminary work, we report on the production of a "standard" siloxane scintillator, added with a suitable combination of primary dye and wavelength shifter, where ^{6}LiF nanocrystals have been embedded. The choice of LiF as lithium bearing compound is dictated by several key features, such as minimal molecular volume, higher Li mass % content as compared to other Li salts and negligible hygroscopicity, which induces opacity and, in turn, severe light output loss. The critical issue to be addressed is the addition of ^{6}LiF to the siloxane matrix while preserving the light output. Therefore, the entrapment of nanoparticles, which are known to minimize light scattering effects, has been herein exploited for the first time. The synthesis of the nanocrystals of ^{6}LiF has been pursued by two different routes: the co-precipitation method in a water:ethanol solvent:co-solvent system [9] and the high temperature decomposition of trifluoroacetate lithium precursor (LiTFA) in oleic acid/octadecene environment [10].

2. Materials and methods

Polysiloxane based scintillators are obtained by Pt catalyzed addition reaction, as described previously [4,5]. In case of scintillators, one can add suitable dyes and neutron converter to the base resin, before vulcanization. In this case, 2,5-diphenyloxazole (PPO) was chosen as primary dye and Lumogen Violet (Basf, LV) as wavelength shifter.
As neutron absorber ^{6}Li was chosen because of its unique and clean decay channel consisting of a 2.73 MeV triton and 2.05 MeV alpha particle, as mentioned above. Among the various lithium compounds, lithium fluoride displays the lowest water absorption and, very recently, LiF nanoparticles synthesis has been reported [9,10]. In this work, ^{6}LiF nanoparticles were prepared using two different methods: co-precipitation and thermal decomposition of ^{6}LiTFA. In the first process, ^{6}Li chloride was prepared from hydrated ^{6}Li oxide, by treating the suitable amount in a pyrex capsule with hot concentrated HCl acid. Hence, the white salt was dissolved in a fixed volume of water:ethanol mixture to obtain a 0.2 M solution. Then it was slowly added to an already prepared solution of NH_4F in the same concentration and volume of solvent:co-solvent. The reaction was continued for about 1h, then the nanocrystals were collected by centrifugation.
In the other method, the preparation of ^{6}LiF with a shell of oleic acid, hereafter called ^{6}LiF OA, started from ^{6}LiTFA, obtained by treating hydrated ^{6}Li oxide with hot trifluoroacetic acid. Then, ^{6}LiTFA was mixed with oleic acid and octadecene (1:1 mixture) and the solution was heated under argon at 320°C for 1h. After cooling, excess ethanol was added and the nanocrystals with oleic acid functionalization were recovered by centrifugation.
Samples of polysiloxane with added ^{6}LiF were prepared with amounts of 0.5, 1 and 2 wt% of ^{6}Li by simple dissolution of oleic acid-capped particles, while mechanical blending was applied to disperse the nanoparticles from co-precipitation (water:ethanol 0:1). The samples with ^{6}LiF obtained from co-precipitation show several small undispersed grains, demonstrating the insolubility of the powders inside the siloxane matrix. On the other hand, ^{6}LiF OA containing samples, which are about 0.5 mm in thickness, appear as homogeneous, though as the amount of ^{6}LiF increases the optical clarity decreases remarkably. Samples with 0.5% of ^{6}Li were also obtained with different thickness (0.5, 1, 2 and 5mm). Only the samples containing ^{6}LiF OA have been tested with alpha and neutrons, since the other samples set cannot afford reproducible results.
Scintillation measurements were made by exciting the samples with a ^{241}Am α source, with a ^{60}Co γ-rays source and with a neutron AmBe source. Pulse height spectra were obtained by coupling the scintillator samples to an H6524 Hamamatsu PMT and wrapping them with aluminized Mylar on the front-face and Teflon tape on the side walls in order to maximize the light collection. In the case of neutron test, the AmBe source was shielded with polyethylene (6 cm) and lead (1 cm) bricks in order

to moderate neutrons and to block γ-rays. The yields were compared with that obtained from EJ-212 plastic scintillator (Eljen Technology Products, 1 inch diameter, 1 mm thickness) and lithium glass GS20 (Applied Scintillation Technologies, 1 inch diameter, 1 mm thickness) in the same experimental conditions.

3. Results and discussion

In figure 1 SEM images of the powders obtained by co-precipitation are shown. When equal amount of water and ethanol is used, micron sized cubes, highly regular with a quite narrow size distribution are produced. If only ethanol is used, the particles are much smaller and their size decreases down to some hundreds of nm.

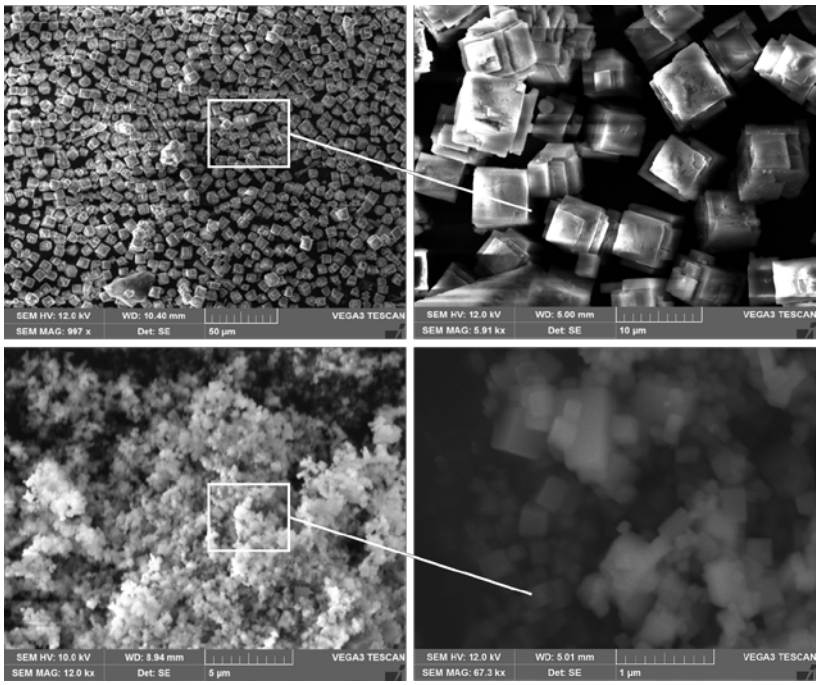

Figure 1. SEM images of 6LiF crystallites obtained using different ratios water:ethanol (top panel 1:1, bottom panel 0:1).

In the case of LiTFA decomposition, SEM inspection evidences flower-like structures, as visible in figure 2. Oleic acid may promote aggregation of nanocrystals during growth at high temperature, with formation of different shapes and size in the order of some microns.

High-resolution X-ray diffraction analysis has been performed on powders (figure 3). All the samples show the typical XRD pattern of crystalline LiF (griceite). As for the particle size, the FWHM of the main peak (200) can be observed for a qualitative comparison. A slight peak broadening is visible for the case of co-precipitation synthesis as the amount of water decreases, indicating a smaller crystallites size. The peak width of ^{6}LiF OA sample is quite similar to the other cases and from the Scherrer formula, the crystallites size has been estimated to about 25 nm.

The samples with ^{6}LiF OA have been tested under alpha irradiation and the results are reported in figure 4 (left). As compared to EJ212, the light output reaches high values, up to 80% of EJ212, almost the same value of GS20. Sample thickness detrimentally affects the light collection, owing to reabsorption effects, as can be seen from light output decrease for increasing thickness. The energy resolution, estimated on the basis of the full width at half maximum (FWHM) of the peak, accounts for small deviation from this general behaviour. Nonetheless, in spite of its low transparency, the sample 5 mm thick still displays a moderately high light output (about 50% of EJ212).

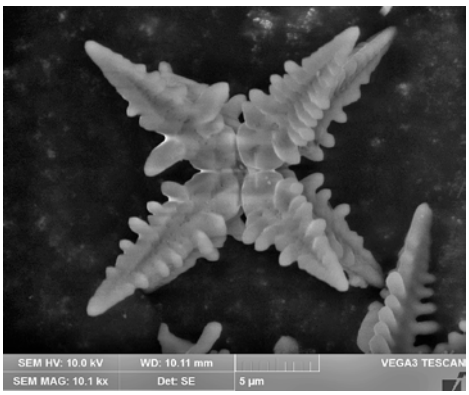

Figure 2. SEM image of ^{6}LiF OA capped aggregate.

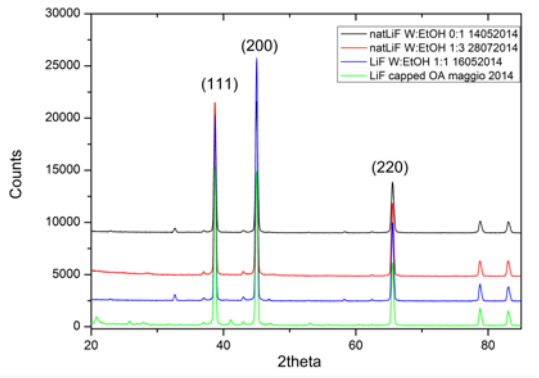

Figure 3. HR-XRD patterns from powders synthesized by the two different pathways.

Exposure to thermal neutrons allowed to record the spectra of figure 4 (right side), where the spectra from samples with 0.5% ^{6}Li and different thickness are reported and compared with GS20 standard. The samples spectra were collected with double gain with respect to GS20 as set on the amplifier. The response of GS20 appears as composed of more than one component (inset graph in figure 4, right panel). This can be ascribed to edge effects, where the produced ionizing particles, either alpha or triton, escape from the disk borders with incomplete energy deposition. However, the observed behaviour is still under discussion. The 0.5 mm thin samples obtained by adding higher amount of ^{6}LiF produced very low response to thermal neutrons, owing to the severe lack of transparency and low active volume for neutron capture. On the other hand, ^{6}LiF OA (0.5 wt%) dissolved in siloxane based scintillator with thickness 2 mm and 5 mm displayed a good response in light output, in spite of the quite low transparency of the latter (photos in figure 4).

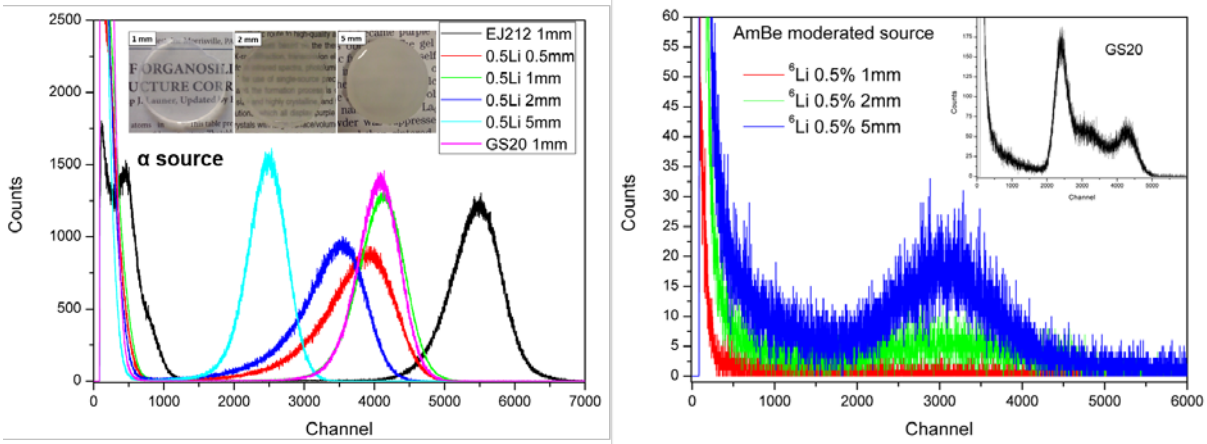

Figure 4. Pulse-height spectra collected by exposing the samples with 0.5 wt% 6Li and different thickness to alpha particles (left) and thermalized neutrons (right). Photos of the samples are reported in the inset on the left, while the neutron spectrum from GS20 is in the inset on the right, for the sake of clarity.

Neutron absorption within a scintillating material is described by the exponential attenuation of the impinging neutron beam, when passing through the material. The attenuation level depends on the absorbing nucleus concentration, its capture cross-section and the thickness of the absorbing layer. The neutron absorption length l is defined as the material thickness necessary to attenuate the original fluence of the impinging neutron beam down to a factor $1/e$ (i.e. about 63% absorption) [1]. In the case of GS20, which contains higher amount of ^{6}Li (1.6×10^{22} at/cm^{3}) and has higher density (2.5 g/cm^{3})

than our 0.5 wt% loaded samples (^{6}Li 5×10^{20} at/cm^3, density 1.03 g/cm^3) the absorption length is about 0.7 mm for thermal neutrons, while in the case of siloxane is about 20 mm. Therefore, it can be inferred that the higher thickness in siloxane based samples accounts for higher peak intensity and better signal-to-background ratio in the pulse-height spectrum, as visible in figure 4. On the other hand, the simple approach of increasing thickness to get still enhanced active volume for capture and, in turn, improved neutron sensitivity is not straightforward. In fact, the light pulse generated by the ionizing particles from the capture reaction (alpha and triton) must travel through the material until reaching the PMT window and self-absorption can severely hamper this process. Thicker samples should be prepared to get insight on the upper limit in thickness where light transport limitations counterbalance the larger capture volume.
Another interesting aspect is the γ-rays background, visible as a shoulder in the low channels region, which derives from the AmBe source not completely shielded. The thicker the sample the more significant becomes the contribution from Compton interactions. Nevertheless, the neutron signal is clearly well separated from the shoulder due to γ-rays background, thus indicating that n-γ separation is possible simply on the basis of pulse height discrimination.

4. Conclusions

^{6}LiF nanoparticles have been synthesized both by co-precipitation and ^{6}LiTFA thermal decomposition in oleic acid environment. In the first case, ^{6}LiF nanoparticles with variable size have been obtained controlling the ratio between solvent and co-solvent. However, the entrapment of the nanocrystals into the siloxane matrix produced non homogenous pellets, with visible granules and agglomerates. On the other hand, ^{6}LiF crystals synthesized with a cap layer of oleic acid proved to be compatible with siloxane matrices. Samples with different thickness and loadings of neutron absorber have been prepared, bearing moderate solubility and optical clarity. Test with neutrons from a moderated AmBe source demonstrated that, in spite of the low content of ^{6}Li, siloxane based scintillators can be used to detect thermal neutrons, as proved by the appearance of the capture peak in the pulse height spectrum, provided that the scintillator thickness is high enough to capture a good fraction of impinging thermal neutrons, but low enough to limit light loss by self-absorption.

Acknowledgments

Authors are very thankful to Mr Selvino Marigo and Mr Alessandro Minarello for their precious technical work. This work has been financially supported by INFN Commission IIIrd and Vth and by the Ministry of Education Education (Prin 2010-2011 -2010TPSCSP_005- *Developments of new detectors and analysis techniques for experiments with radioactive beams at the National Laboratories of INFN, with special reference to the SPES project*).

References

1. Van Eijk CWE, Bessiere A, Dorenbos P, 2004 *Nucl. Instrum. Meth.* A **529** 260.
2. Zaitseva N, Newby J, Hamel S, Carman L, Faust M, Lordi V, Cherepy N, Stoeffl W, Payne S, 2009 *Neutron detection with single crystal organic scintillators*, Proc. SPIE 7449.
3. Bell ZW, Brown GM, Ho CH, Sloop FV, 2003 *Organic scintillators for neutron detection*, Proc. SPIE 4784.
4. Carturan S et al., 2011 *Rad. Prot. Dosimetry* **143** 471.
5. Carturan SM, Marchi T, Fanchini E, De Vita R, Finocchiaro P, Pappalardo A., 2014 *Eur. Phys. J. Focus Point* **129** 212.
6. Barbagallo M et al., 2013 *Rev. Sci. Instrum.* **84** 033503.
7. Quaranta A et al., 2011 *J. of Non-Cryst. Solids* **357** 1921.
8. Knoll GF 1979 *Radiation Detection and Measurement* (John Wiley & Sons, Inc., New York), chapter 14 p 519.
9. Alharbi ND, Salah N, Habib SS, Alarfaj E, 2013 *J. Phys. D: Appl. Phys.* **46** 035305.
10. Du Y-P, Zhang Y-W, Sun L-D, Yan C-H, 2009 *Dalton Trans.* **40** 8574.